NOVA
SCIENCE PUBLISHERS, INC.

THE VARIABLE SOLAR DYNAMO AND THE FORECAST OF SOLAR ACTIVITY; INFLUENCE ON TERRESTRIAL SURFACE TEMPERATURE

C. De Jager
S. Duhau

In: "Global Warming in the 21st Century"
Editor: Juliann M. Cossia
ISBN: 978-1-61728-980-4 2011

400 Oser Avenue, Suite 1600
Hauppauge, N. Y. 11788-3619
Phone (631) 231-7269
Fax (631) 231-8175
E-mail: main@novapublishers.com
http://www.novapublishers.com

In: Global Warming in the 21st Century ISBN 978-1-61728-980-4
Editor: Juliann M. Cossia

Chapter 3

THE VARIABLE SOLAR DYNAMO AND THE FORECAST OF SOLAR ACTIVITY; INFLUENCE ON TERRESTRIAL SURFACE TEMPERATURE

***C. De Jager*[*1] *and S. Duhau*[2]**
[1]Royal Netherlands Institute for Sea Research;
1790 AB Den Burg, The Netherlands
[2]Departamento de Física, Facultad de Ciencias Exactas y Naturales,
Universidad de Buenos Aires, 1428, Bs. As

ABSTRACT

Solar variability is governed by the solar dynamo, an intricate interplay between the sun's poloidal and toroidal magnetic field components. The most pronounced periodicity is the Schwabe cycle of about 11 years duration, and the Hale cycle, consisting of two successive Schwabe cycles. Another important cycle, with variable length, is named after Gleissberg. We describe the role of the two magnetic field components in these periodicities and forward suggestions for the solar mechanisms at work in driving these. We suggest that the Hale cycle is due to magnetohydrodynamic oscillations of the tachocline with a period of about 22 years. The time-behaviour of the longer components, along with information on the phase-relationship between them allows us to forecast the solar future behaviour. We expect a low next solar maximum, around 2014. After the 20th century's Grand Maximum, a Grand Minimum will start in one or two decades from present. It will last for at least one Gleissberg cycle. We describe the correlation of the two solar magnetic field components with terrestrial surface temperature variations for the period 1610 to 1970. About 40% of the gradual increase of terrestrial surface temperature is correlated with solar variability. Of this amount about two-thirds is correlated with toroidal field variations and that component can fully be explained quantitatively by the gradual increase of Total Solar Irradiance and the consequent feedback by evaporated gases. A yet unexplained fraction of ~30% is correlated with the poloidal field. After subtracting these components the residual smoothed global warming was 0.31 degrees in 1999.

* Email: *cdej@kpnplanet.nl*

1. INTRODUCTION

This paper summarizes and reviews our recent investigation in the field of solar and solar-terrestrial physics and it partly elaborates details. We first describe the conventional periodicities in solar variability: the Schwabe, Hale, Gleissberg, De Vries (Suess) and Hallstadt cycles. A particular aspect of solar variability is the Grand Episodes of which three types are identified: Grand Minima, Grand Maxima and episodes of Regular Oscillations. All aspects of solar variability find their basis in the tachocline, the region at the basis of the outer solar convection zone, about 200,000 km below the surface where, by interaction between the convection and the differential solar rotation, strong electric currents originate that lead to the formation of strong magnetic fields that, after having detached and risen to the surface, manifest themselves in the various aspects of solar variability: spots, facular fields, flares, coronal mass emissions, coronal holes, polar bright points, polar faculae, just to mention the most important aspects. The fields in the tachocline lead to the origin of a toroidal and a poloidal magnetic field. This complex of activities forms the solar dynamo. We describe the proxies that are needed to obtain information on these fields. Their analysis leads to the identification of the various types of periodicities mentioned in the beginning of this section. It also allows one to forecast the next solar cycle, its year of maximum and its amplitude expressed in sunspot numbers. A plot of one of these two proxies against the other leads to a phase diagram with a good diagnostic value. It shows that the 20^{th} century's Grand Maximum has just ended and the phase diagram allows us to define the character of the next Grand Episode. Both the earth's global surface temperature and most of the relevant solar variables have increased gradually over the last four centuries. This information makes possible to determine the correlation between surface temperature and the two magnetic components of the dynamo. It also leads to a prediction of the temperature decrease associated with the forthcoming Grand Minimum.

2. SOLAR PERIODICITIES

There exists a vast literature on solar periodicities or quasi-periodicities. Most of them have been derived on basis of Fourier-type analyses of sunspot numbers or of data on the flux of cosmogenic radionuclides. The question is relevant what kind of solar observed phenomena should be used for such analyses. Conventionally, these periodicities are called 'cycles' and we will stick to that tradition in this Section, though realizing that a physically based definition of these (quasi-) periodicities would be in place. We return to this matter in Section 10 of this paper.

Solar variability shows itself best by the sunspots because these are easily visible even with fairly primitive means. But the spots are just one of the reflections of the activity of the solar dynamo, which is a dynamic complex that finds its origin far underneath the solar surface. Sunspots are by no means comparable, neither in intensity or dynamism nor in energy yield, with phenomena such as the solar flares, the coronal mass ejections, the polar facile and bright spots, not even with the facular fields surrounding the spots. Spots are that quiet and inactive because of their strong magnetic fields that halt convective motions. Hence one may wonder if sunspots are a good measure of solar variability, but sunspot observations

are available for four centuries, hence they are a suitable indication for solar activity. Also, since quantitative data on periodicities are mainly derived from records of sunspot counts the following summary of periodicities relies for the most part on sunspot data.

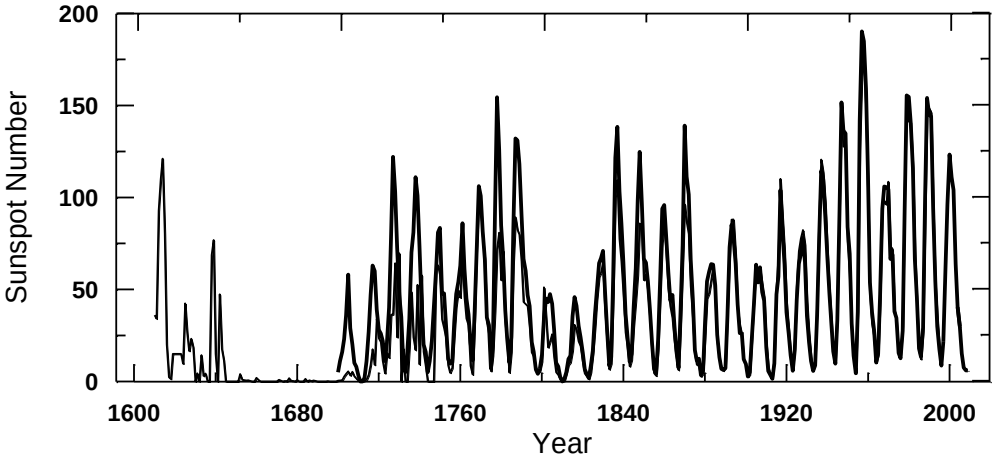

Figure 1. Sunspot numbers from 1610 – 2000. The diagram shows the Schwabe cycles. Note the impressive Maunder minimum in the second half of the 17th century and the likewise impressive Grand Maximum of the 20th century. The Dalton Minimum is around 1810.

An extensive overview of solar cycles was published by De Jager (2005), pp. 232 - 234. We summarize, while neglecting those cycles that seem not to be of solar origin:

The most pronounced cycles are the Schwabe and Hale cycles of average 11 and 22 years durations. They are not constant; neither in duration nor in amplitude (cf. Figure 1). The length of the Hale cycle was 22.9 yr before the Maunder Minimum (1650 – 1720). During that Minimum the period was 24 and 15.8 years and thereafter it increased to 26 yrs (Raspopov et al., 2004). The Hale cycle shortened to about 21 yrs during the Grand Maximum of the past century.

There is a periodicity of 1.3 yrs in the solar rotation rate that reflects itself in the sunspot numbers and in the areas of sunspots (Bazilevskaya et al., 2000). Benevolenskaya (2003) found that it varies between 1.0 and 1.3 years. Krirova and Solanki (2002) suggest a relationship between the 1.3 yrs and the 156 days cycles (the 'Rieger period') in the frequency of enhanced solar flaring. They mention that 156 days is a third harmonic of 1.3 years. Along that line one may wonder if the 1.3 ± 0.2 yrs cycle is a high harmonic of the Schwabe cycle because 8 x 1.3 = 10.5, which was the length of the Schwabe cycle during the past Grand Maximum.

On the basis of only 200 years of available observations Gleissberg (1944, 1958) found a cycle of ~ 80 years in the amplitude of the record of sunspot numbers. Later investigations confirmed its reality. Damon and Sonnett (1991) and Damon and Peristikh (1999, 2000), using ^{14}C records, could trace it back over the Holocene, till 11,600 years before 1950. They found an average period of 87.8 years but in subsequent research Ogurtsov et al. (2002) concluded that there is a wide frequency band with a double structure; one of 50 – 80 years and another of 90 – 140 years. A Fourier analysis of sunspot numbers over the past 400 years gave average periods of 53 and 101 years (Le and Wang, 2003). The 101 years period had its largest amplitude around 1850 and the 53 years period was chiefly active between 1725 and

1850. These results might seem questionable since they were based on a short time basis but subsequent research by Raspopov et al. (2004) confirmed that the shorter period did prevail between 1725 and 1850. They add that after 1760 the average Gleissberg period increased to 90 – 100 years.

The De Vries (or: Suess) period of 205 years is observed in ^{14}C and ^{36}Cl records. Muscheler et al. (2003, 2004) gave 205, 208 and 207 years. Wagner et al. (2001), Tobias et al (2004) determined the period at 205 years. It is a fairly sharp period with little or no variability. Ogurtsov et al. (2002) found it to be single peaked in the 170 – 260 years band.

Finally, we mention the Hallstadt periodicity of ~ 2300 years (Cliverd et al., 2003). Its reality was confirmed by Muscheler et al. (2003).

The solar origin is obvious for the Rieger, Schwabe, Hale and Gleissberg cycles but it seems also true for the De Vries and Hallstadt cycles. We conclude that there are six fairly well founded cycles in solar activity. They are named after Rieger, Schwabe, Hale, De Vries (Suess), and Hallstradt. Some uncertainty exists on the Rieger periodicity and its harmonics.

3. THE SCHWABE AND HALE CYCLES. THE BUTTERFLY DIAGRAM AND ITS EXTENSION

In 1843 the amateur-astronomer Schwabe discovered that there is an 11 years periodicity in the number of sunspots. The Schwabe cycle is now known from 1610 onward, the year of first telescopic observations of the sun. A plot of sunspot number R against time shows the variable character of successive sunspot cycles (Figure 1). Interesting is cycle nr. 4, which seems remarkably long. Actually it consists of two shorter cycles (Usoskin et al., 2009).

In 1908 Hale at Mt Wilson found that two successive Schwabe cycles are complimentary according to their magnetic character. The Hale-Nicholson polarity laws state that while in the one cycle the leading spots of spot groups at the northern hemisphere have north polarity while the reverse is true at the other hemisphere, that situation changes into the opposite during the next Schwabe cycle. Also, the polar fields change sign every Schwabe cycle. Hence, it makes sense to introduce the Hale cycle, consisting of two Schwabe cycles. The question then arises: which of the consecutive Schwabe cycles form a Hale cycle – in other words: does a physical connection exist between successive Schwabe cycles. This was answered by Gnevishev and Olh (1948) who found that observables in even cycles and the following odd cycles are much stronger correlated that those with the preceding odd cycle (correlation coefficients 0.91 and 0.50, respectively)

Additional physical information is given by a plot of the heliophysical latitudes of appearance of sunspots. It then appears that the first spots of a cycle appear at relatively high latitudes ($\sim 35^o$) while those spots that originate later during the cycle are found at increasingly lower latitudes (Figure 2). This *butterfly diagram* makes clear that in the course of a cycle the location of the activity centres tends to decrease in latitude, moving to the solar equator.

It is essential to consider the polar magnetic activity as well. It can best be measured through the coronal line intensities measured along the sun's limb with coronagraphs. The 'green' coronal 5303 Å line is mainly emitted by gas in the so-called coronal condensations which is dense plasma confined by closed magnetic fields. Hence, their study yields

information on closed magnetic fields above the solar photosphere. The polar observations, when added to the butterfly diagram (Figure 3), yield important additional information on the mechanisms at work in solar activity. The diagram proves that magnetic fields first appear in polar areas while gradually moving towards the equator (Callebaut and Makarov, 1992; Makarov and Makarova, 1999; cf. also Makarov et al., 2010).

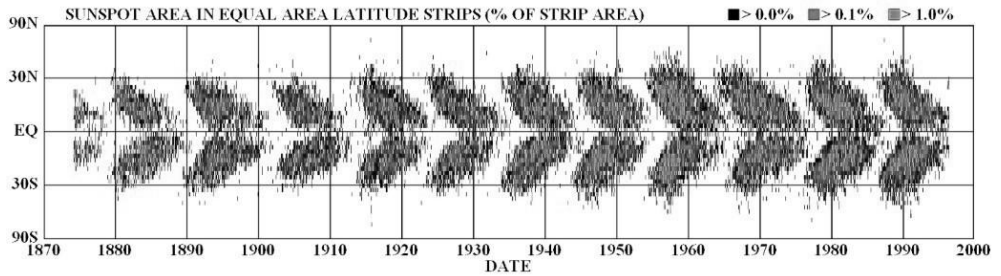

Figure 2. The Maunder or butterfly diagram. From Hathaway, NASA. First spots of a cycle appear at high latitudes. The average latitude of appearance decreases in the course of the cycle.

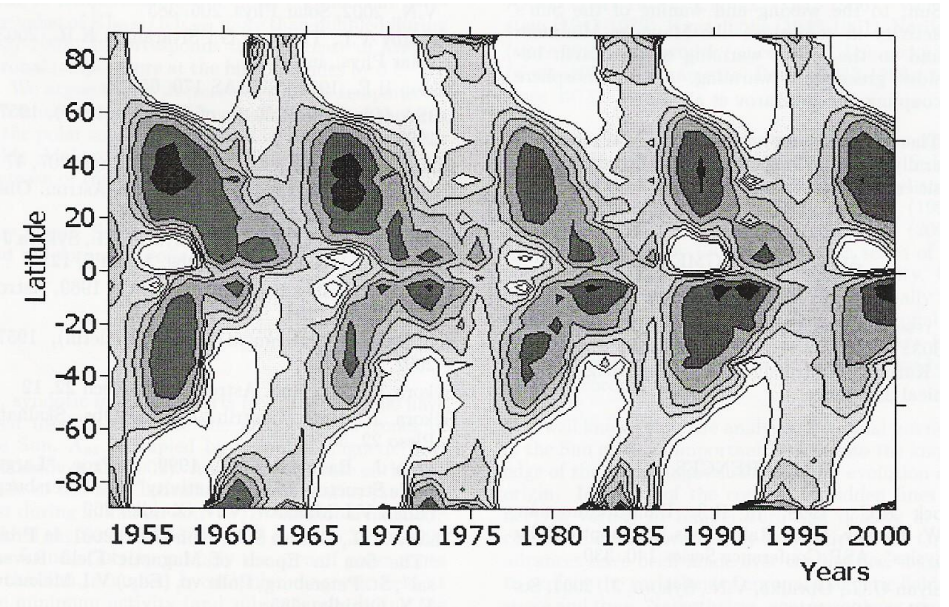

Figure 3. 'Extended' butterfly diagram based on coronal observations. (Makarov and Makarova, 1999).

It also shows that polar activity is in antiphase with the equatorial one. At maximum sunspot activity the polar activity has its minimum values and the reverse is true at minimum sunspot activity. We bring this in connection with the finding by Gnevishev and Olh (1948), that the even cycles are best correlated with the subsequent odd one. This has implications for our understanding of the solar dynamo, because it leads to the conclusion that the deep-seated pulsation activity that regulates solar variability, consists of the 22-years pulsations of the tachocline during an even and subsequent odd cycle. Hence, Schwabe cycles # 22 and #23

form a physically connected couple, as will be the case with #24 and #25. See further Section 7.

An aspect that is not generally known is that the total flux from the polar faculae is several times the total sunspot flux (Callebaut and Makarov, 1992), which is a reason for not neglecting the polar magnetic fields in discussions of solar activity and sun-climate relationships.

4. GRAND EPISODES

A glance at the sunspot cycle (Figure 1) shows that not all cycles are the same, neither in intensity nor in duration. This is partly related to the cyclicity mentioned in Section 2, but on top of that there are more conspicuous episodes. The most dramatic one is the Maunder Minimum named after the Maunder couple, who were the first to mention it (cf. Eddy, 1976; Soon and Yaskell, 2003). The Maunder Minimum is the period 1640 – 1720 during which there were virtually no spots visible on the sun. In contrast to that stands the Grand Maximum of solar activity of the 20th century which was extreme in numbers of sunspots.

Sunspots were only observed on a semi-regular basis after the invention of the telescope and its first use for astronomy by Galileï. But cosmogenic nuclides, mainly those of ^{10}Be are important means for going backward over many centuries, even before 1610. Figure 4, after Usoskin et al. (2003) shows solar variability since the year 850. The diagram is dominated by a few characteristic 'grand episodes' of which three kinds have been identified so far (Duhau and De Jager, 2008).

One of these is the *Grand Minima*, named after Oort, Wolf, Spörer, Maunder. A smaller and shorter minimum in the early part of the 19th century is called after Dalton. We do not rank it among the grand episodes. It is part of the episode that we (Duhau and de Jager, 2008) called the episode of Regular Oscillations. Its origin may differ from that of the grand episodes (cf. also our remarks to that end in the last paragraph of Section 9).

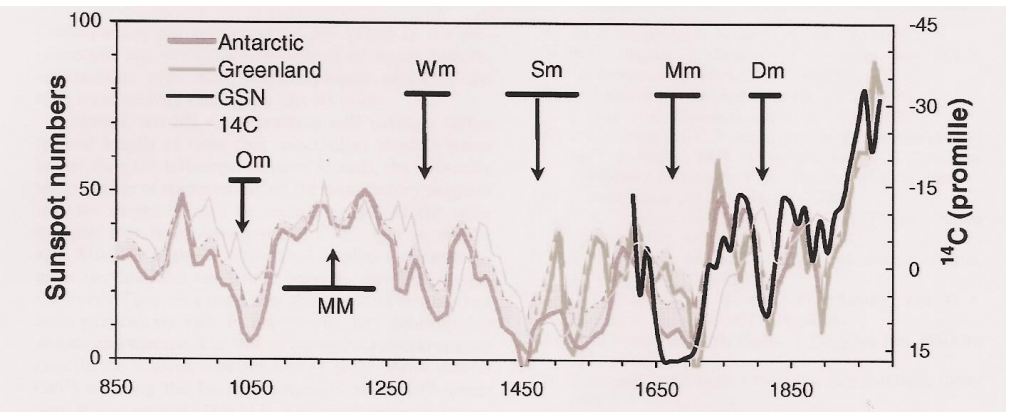

Figure 4. Grand Episodes in solar activity: the Oort, Wolf, Spörer, Maunder and Dalton Minima and the Medieval and 20th century Grand Maxima. The thick solid line is the sunspot numbers, the others are based on fluxes of cosmogenic radionuclides (diagram from Usoskin et al, 2003).

Next to that, the diagram shows two *Grand Maxima*: the Medieval Maximum and the 20th century Grand Maximum. It should also be noted that there are differences between the sunspot record (thick solid line after 1610) and those based on cosmogenic radionuclides. While the number of spots was very small during the Maunder Minimum, the ^{10}Be record shows a slightly different behaviour. This is related to the other heliophysical origins of sunspots and of the plasma clouds that influence the cosmic ray flux bombarding earth. Later in this paper (particularly Section 9) we return to this important difference, which is fundamental if one would wish to understand why there are differences between equatorial and polar activity, particularly in their role for terrestrial surface temperatures.

A third type of Grand Episodes is the *Regular Oscillations* (Duhau and De Jager, 2008). These are oscillations of the Gleissberg-type component of solar variability, with a quasi-regular character, around the average level of solar activity. The most recent and therefore best studied example is the period 1724 – 1924.

5. THE TACHOCLINE

The tachocline is the seat of the solar dynamo, where solar variability originates. It is the region where in dynamo theories toroidal magnetic fields are generated by strong electric currents. These magnetic fields may detach from the global field pattern and thereupon they may rise buoyantly to appear at the surface as a pair of sunspots.

The tachocline is the "thin transitional layer below the solar convective zone between the surface-like differential rotation pervading the convective zone and the rigid rotation of the solar interior" (Forgács-dajka and Petrovay, 2002). By defining its 'full thickness' as the radial interval over which the horizontal differential rotation is reduced by a factor 100 (Forgács-dajka and Petrovay, 2001) these authors find a value of 0.04 ± 0.014 R_o. They conclude that it is centred at $0.691R_o$, which is directly beneath the convection zone of which the lower limit is at 0.0713 R_o. Kosovichev (1996) finds essentially the same value, 0.692, for the central position of the tachocline. There are indications for a slightly prolate form of the tachocline; at 60° latitude the centre being situated at 0.71 R_o. Hence it penetrates into the convective region at high latitudes. At lower latitudes, which are the latitudes where sunspots and Active Regions are generated, the tachocline is at the location of the downward overshoot layer of the convective region, hence at the lower border of the convection zone proper.

Stability analyses show that toroidal flux tubes can only survive for a period comparable to that of the Hale cycle (a necessary condition for explaining solar sunspot variability) in the region *below* the unstably stratified part of the convection zone (Gilman and Dikpati, 2000; Gilman, 2000). This is the importance of the tachocline (Moreno-Insertis, 1994). Its thinness implies anisotropic transport of angular momentum (Spiegel and Zahn, 1990).

Since the tachocline is the seat of the dynamo it is important to know its equipartition magnetic field. A simple estimate based on $B^2 = 4\pi\rho(\Delta v_{shear})^2$ yields values of the order of 2×10^3 Gauss. A more elaborate treatment, based on the balance between magnetic and Coriolis stresses (Ruzmaikin, 2000), yields 8.7×10^3 Gauss, hence roughly 10^4 Gauss. Later we will show that the buoyancy of sunspots demands the local and temporal occurrence of fields of 10^5 Gauss, a requirement that demands super-equipartition. This is indeed possible as demonstrated by Caligari et al. (1995).

Another value of importance is that of the magnetic diffusivity η. It enters the present discussion through the reasonable hypothesis that the Hale cycle is due to an oscillating magnetic field in the tachocline. The assumption that the tachocline is the seat of the 22-years cyclic periodicity is supported by, first, the finding that the convective envelope cannot be the seat of a large-scale ordered dynamo with that long periodicity (Brun, 2004). Additional support is the observation (Akasofu et al., 2005) that the active longitudes (cf. our more detailed description in Section 7) can be represented by two dipole fields at 180° separation that vary in strength during the Schwabe cycle. This finding perfectly visualizes the hydromagnetic oscillations of a magnetic flux tube situated in or near the tachocline.

Such an oscillating magnetic field penetrates a conductive medium down to a skin depth $H = (2\eta/\omega)^{1/2}$. Assuming the molecular value for the magnetic diffusivity and taking a period $P = \omega/2\pi$ = 22 years, one finds a depth of only a few km (Petrovay and Forgács-dajka, 2003). But in order to store a toroidal magnetic field of 10^5 Gauss, a value needed for buoyancy, the storage region must have a thickness of at least several thousands of km, which is of the order of at least one-tenth of the thickness of the tachocline (Forgács-dajka and Petrovay, 2002). A turbulent magnetic diffusivity of at least 10^9 cm^2 s^{-1} would therefore be needed. We note in passing that the requirement that the penetration depth is *equal* to the *thickness of the tachocline* demands that η should be of the order of 10^{11}.

Inside the convection zone, where turbulence is strongly developed, the turbulent magnetic diffusivity η is of the order of 10^{13} ((Forgács-dajka and Petrovay, 2001, 2002) and one would expect smaller values in the overshoot layer that constitutes the tachocline. Nandy (2002) calculated the buoyant eruption in the toroidal belt for different values of η and concluded that its value should be 7.5×10^{10} cm^2 s^{-1}. In his paper he refers to Parker (1993, with reference to other authors) who determined magnetic diffusivity and who too found values of order 10^{10} to 10^{12} cm^2 s^{-1}. Also Petrovay and Forgács-dajka (2003) find that model calculations require a value of 10^{10} cm^2 s^{-1}. Dikpati et al. (2004) determines values of 10^{10} to 10^{11}at the tachocline level. They increase to higher values higher-up in the convection zone. We are therefore inclined to assume these values as a reasonable compromise; the precise value is not too critical. We note that this value corresponds – as order of magnitude is involved – to equalising the skin depth to the tachocline thickness.

One *conclusion* is therefore that the most likely value for the magnetic diffusivity favours a model in which the solar sunspot cycle is governed by a periodic magneto-hydrodynamic pulsation of the tachocline with a period of about 22 years. Another consequence of the high (turbulent) magnetic diffusivity is that the dynamo field dominates the dynamics of the tachocline process (Forgács-dajka, 2000, and many other authors).

6. FAST OR SLOW TACHOCLINE/DYNAMO – DOES IT REQUIRE A RELIC INTERIOR FIELD

Existing theories distinguish between a fast and a slow tachocline (alternatively formulated: a fast or slow dynamo). In case of a fast tachocline/dynamo the processes are governed by an oscillatory magnetic field in the tachocline, on Hale-cycle time scales. In the other case the dynamo field cannot penetrate into the tachocline and one has to assume that a deeper seated internal (relic) magnetic field penetrates into the tachocline. Petrovay and

Forgàcs-dajka (2003) state that the poloidal field for the slow tachocline is uncoupled from that in the convective envelope and that the fast one should be coupled. However, that would be true if only diffusive coupling is assumed, but a convective mixing is possible between the tachocline and the convective envelope as is assumed, instead, in some dynamo models. The 'fast tachocline' model avoids the need of a relic field from the radiative interior, as would be needed in the case in the 'slow tachocline' models. Hence it is crucial to discuss the existence of a relic field in the solar interior.

Helioseismologic observations have yielded good information on the internal solar rotation. The inner, radiative part of the sun, up to a level, slightly below the basis of the convection zone, shows solid body rotation while the convection zone shows latitude-dependent differential rotation. The question we want to study here is if there is a magnetic field in the radiative interior, and what is its strength and structure.

Cowling (1945) was the first to suggest that a relic dipole field may exist in the radiative core. It would persist over the life time of the sun because of the high electric conductivity of the solar plasma and because of the its dimensions. The Gnevyshev-Olh (1948) odd-even rule was attributed by Sonett (1983) to the presence of this relic dipole field. From observations of the direction of the heliomagnetic equator in the interval 1976-1992 it was found (Bravo and Steward, 1995) that variations of that direction may be explained by the presence of a relic polar field pointing southward, tilted with respect to the solar rotation axis to form an angle of 72º with respect to the solar equator. In that line several authors (Mestel and Weiss, 1987; Charbonneau and McGregor, 1992) have shown that a large-scale poloidal field suffices to redistribute initial differential angular rotation in such a way as to accomplish uniform rotation in the radiative region. The value of the field is not very critical. Charbonneau and McGregor (1993) who made a series of numerical evolutionary calculations for assumed poloidal fields in the range between 0.01 to 10 G found that such fieldstrengths are sufficient for establishing uniform rotation. According to the calculations the weaker potential fields, with fieldstrengths below 1 Gauss, will penetrate into the convection zone. Such fields would dissipate in a time span shorter than the solar lifetime (Friedland and Gruzinov, 2003). Hence, this criterion sets a lower limit of ~ 1 Gauss to the strength of the poloidal field that would be needed to inhibit differential rotation in the radiative solar interior. This conclusion may be compared with one from Charbonneau and McGregor (1993), who found, from comparison of observations with their theoretical calculations, that these favour a magnetically uncoupled poloidal configuration with fieldstrengths of the order of one Gauss.

Evolutionary calculations (Charbonneau and McGregor, 1993, cf. also Ruzmaikin, 2000) confirm that such fields are persistent and have a lifetime that exceeds that of the Sun. Overall, however, the present internal solar rotation is "a poor indicator of any large-scale poloidal magnetic field present in the radiative interior of the Sun" (Charbonneau and McGregor, 1993).

Hence the internal poloidal field is likely to be a relic poloidal field, of the order of at least one Gauss, to perhaps a few tens of Gauss. Its importance is that it may be at the basis of some observed asymmetries in the solar dynamo: the north-south asymmetry, the occurrence of active longitudes and the temporal stability of coronal holes (Song and Wang, 2005).

A toroidal internal field is also possible. Following Bahcall and Ulrich (1971), Friedland and Gruzinov (2003) calculated strengths of an assumed toroidal field and found that toroidal fields of complex spatial structure, persisting over the solar lifetime and not penetrating into

the convection zone are indeed possible. Reversely, an oscillating magnetic field of sufficient strength in the tachocline may penetrate down till into the levels below the tachocline.

A relic field appears to be essentially necessary for having the radiative interior rotating as a rigid body (Charbonneau and McGregor, 1992).

We conclude this Section by summarising that the decision which of the two cases – a fast or a slow dynamo – is actually active in the sun depends on the magnetic diffusivity in the tachocline. For a 'fast' dynamo it should exceed 10^9 cm^2 s^{-1}. We showed in Section 5 that the most probable value is in the range of 10^{10} to 10^{11} cm^2 s^{-1}. Hence we are dealing with the case of a fast tachocline/dynamo. Whether the solar deeper interior has a relic field or not appears not to be important for the present problem, as soon as one assumes a fast dynamo.

7. GENERATION OF TOROIDAL FIELD AND FIELD EMERGENCE; THE Ω EFFECT

In the dynamo model poloidal fields are stretched by latitude-dependent differential rotation and they are thus amplified until the fields get that strong that kink-instable elements detach from the overall tachocline field and rise. That field must arise from an initially weaker poloidal field.

The amplification appears to proceed rapidly. Lillo (2005) assuming a 'shallow water approximation' for the tachocline, found that in an initial phase of its development the strength of an initial seed field grows exponentially. It increases by a factor of the order of 10^2 in about a year. Thereafter it grows slower until equilibrium is reached with the kinetic energy of the surrounding matter. Callebaut and Khater (2006), in a consistent treatment of the involved Lorentz force, calculate a growth rate by two orders of magnitude in a time span of one Schwabe cycle. The field starts with an assumed seed dipolar field. Hence the initial field should be of the order of 1000 G in order to eventually reach 10^5 Gauss. The poloidal field that is at the origin of this process may have originated in the shearing motions in the tachocline. We have shown earlier in his paper that simple equipartition yields that value for the fieldstrength.

An important value is the minimum magnetic fieldstrength needed for buoyancy. If the original field strength is below a few times 10^4 Gauss (≈ equipartition energy) the flux tube can expand catastrophically (Moreno-Insertis et al., 1995). "A rising flux tube with equipartition energy (10^4 Gauss) at their basis explodes in the middle of the convection zone if the magnetic flux is below 10^{21} Mx". Since flux tubes can only be stored inside the tacholine, and in order to remain coherent, their magnetic energy density must be much larger than the kinetic energy of the convective motions. Schmitt et al. (1994) find that the instability arises in the form of growing elliptical waves due to the influence of the Coriolis force. Such a dynamo actually requires such strong field to drive the instability.

The main assumption that leads to very strong magnetic field is the high turbulent diffusivity imposed by the strong oscillatory motions that in turn arise from a strong and fast oscillatory field imposed.

As summarised by Ruzmaikin (2001) buoyancy occurs, in principle, when the field reaches values of the order of 10^4 Gauss. For such relatively weaker fields the Coriolis force $2v\times\Omega$ suppresses the motion at right angle to the axis of rotation, forcing the flux tube to rise,

parallel to the equator. The rise time is calculated at about a month (Caligari et al., 1995). In order to rise rapidly, while not being destroyed by differential rotation, the Coriolis force must be compensated by the radially directed magnetic buoyancy. "For smaller fieldstrengths the field becomes unstable without erupting and can be destroyed by differential rotation" (Ruzmakin, 2001). That occurs when the field at the bottom of the convection zone is about 10^5 Gauss, a value that has been found earlier by Ferris-Mas and Schüssler (1993) and Moreno-Insertis (1994). Basu (1997) even derives a maximum value for the field at the bottom of the convection region of 3×10^5 Gauss.

A value for the limiting field strength can be obtained also from the observed tilt of the line connecting the leading and following spots of a group. That value is 0.6 to 1.6×10^5 Gauss (D'Silva and Chaudhuri, 1993). The precise fieldstrength value depends also on the depth within the overshoot layer and on the angular velocity distribution at that latitude (Ferris-Mas, 2003). A general remark is that there must be a reason why amplification can continue till above the level of equipartition. Forgács-dajka and Petrovay (2002) find a poloidal field at the base of the convective envelop that is too high as compared with the one that is driven by the dynamo. It seems that this is an inconsistency, but several authors have found that over-equipartition is indeed possible. E.g. Caligari et al. (1995) presented calculations showing the possibility of super-equipartition in the overshoot layer.

Such fields are highly kink-instable (Ruzmaikin, 2000):"Toroidal loops rise through the convection zone and erupt at the solar surface to form active regions". Computations show that such field tubes have diameters not exceeding ~ 100 km at the basis of the convection zone. This seems at variance with the observed diameters of the spots but, when rising they expand and show themselves at the surface as a pair of sunspots, with a larger diameter. The ratio between the observed (surface) diameter and that at the bottom, which is about 100, is in accordance with the density ratio between surface and bottom of the convection zone, which is of order 10^4. The calculated rise time is of the order of 3 months which does not differ fundamentally from the one-month rise time derived by Caligari et al. (1995).

The formation of the poloidal fields is therefore an ongoing process that takes place during the whole solar cycle. This conclusion seems inevitable and it therefore leads to the question of the observed periodicity in the appearance of the spots, because that observation seems to contradict the assumption of continuous generation of high fieldstrength tubes in the tachocline.

In this connection attention should be given to the aspect of active longitudes. Active regions seem to prefer appearing at certain discrete longitudes (Neugebauer et al., 2000;

Akasofu et al., 2005). Ruzmaikin et al. (2001), by studying the solar wind find a rotation period of 27.03 d. The active longitudes are separated by 180°. Usoskin et al. (2005) derive rotational velocities of 14.33 and 14.31 deg.day^{-1}. These two values apply to the active longitudes in the northern and southern hemispheres, respectively. This corresponds with an average period of 25.13 deg day^{-1}. Berdyugina et al. (2005) discuss several explanations without succeeding in pin-pointing one of them.

Newly emerging fluxes appear preferably at locations where previously flux has emerged (Gaizauskas et al., 1983). The question arises concerning the physical conditions at these longitudes: is it correct to assume that at such longitudes over-amplification can occur, contrary to other longitudes where these special conditions do not seem to occur? Are these the longitudes of maximum fieldstrength of the pulsating tachocline? There are model calculations available that give a hint to the solution of this problem. There should be a

distribution of the emerging magnetic fields in longitude (Caligari et al., 1995). Ruzmaikin (2001) gives examples of the first two non-axisymmetric modes; that with $m = 2$ shows (evidently) two maxima, separated by 180°. This may have relevance to the observations of active longitudes. Hence, the active solar phenomena can be represented by two hypothetical dipole fields that follow the Hale-Nicholson polarity laws. These dipoles appear to vary in strength during the cycle, showing a pronounced 22 years periodicity (Bravo et al., 1998). We note that this view corresponds to the assumption that solar variability is governed by a periodic magnetohydrodynamic pulsation in the tachocline.

In conclusion, the above considerations suggest a model in which solar variability is due to (semi-)periodic magneto-hydrodynamic pulsation of the fieldstrength in the tachocline. The wavelength of that periodicity should be of the order of the solar circumference. Flux buoyancy occurs at stochastic intervals but successful buoyancy resulting in the appearance of spots is mainly possible at the location of and during periods of maximum fieldstrength of the tachocline. Weaker fields do also detach; but as stated earlier in this paper, these rise mainly into a direction parallel to the rotation axis of the sun to appear in polar regions.

8. VARIABLE LATITUDE OF ACTIVITY; MERIDIONAL CIRCULATION

Consequently, we assume that the solar cycle originates inside the tachocline, where an oscillatory symmetric magnetic dipole is assumed; it oscillates with a period of 22 years. In this model the boundary condition at the bottom, i.e. at the radiative interior-tachocline interface, is that the magnetic field should be zero. The same applies to the tachocline–convective envelope boundary. The model is kinetic: the differential rotation given by helioseismology is assumed and the strength of the field is allowed to rise until a stationary harmonic result is stabilised. In such a way the tachocline is uncoupled from the radiative interior and passively coupled to the convective envelope.

The next question is that of the variable frequency of spots during the cycle because, on the basis of the foregoing, spot occurrence should be a random process, not showing an 11-years distribution in the frequency of occurrence. The answer is found in a remark by Ruzmaikin (2001): Let us assume that a basic oscillation of the tachocline is superimposed by a random distribution in time of the appearance of unstable loops. The combination of the periodically changing fields with the above random component can lead to fields that are strong enough to cross a threshold for rising. Maximum fieldstrengths are reached in two areas at 180^{o} distance along the solar circumference. This model also explains the Hale-Nicholson polarity laws.

The equator-ward drift of the spot zone, as shown by the butterfly diagram (Figure 2) must be caused by a slow meridional circulation; directed equatorward in the relatively deep layers near the tachocline. The inclusion of meridional flow in the dynamo model seems inevitable. Bonanno et al (2002) found from model studies that a model without meridional circulation fails to explain the observations. They add that "a meridional flow with equatorward drift at the bottom of the convection zone of a few meters per second can indeed force the equatorward migration of the toroidal magnetic field". Likewise, the pole-ward motion of the polar filaments (Figure 5) can be understood on the same basis if the latter originate in the higher parts of the convection zone. We mention that the observed poleward

flow in the upper part of the convection zone, as summarised by Dikpati and Gilman (2001, 2007) is 10 to 20 m/sec. *Cf.* also Forgács-dajka and Petrovay: (2002; their Figure 9). In the Dikpati-Charbonneau (1999) computations the flow speed in the upper part of the convection zone is 12 m/s while the magnetic diffusivity was assumed to be $\eta = 3 \times 10^{11}$ cm^2 s^{-1}.

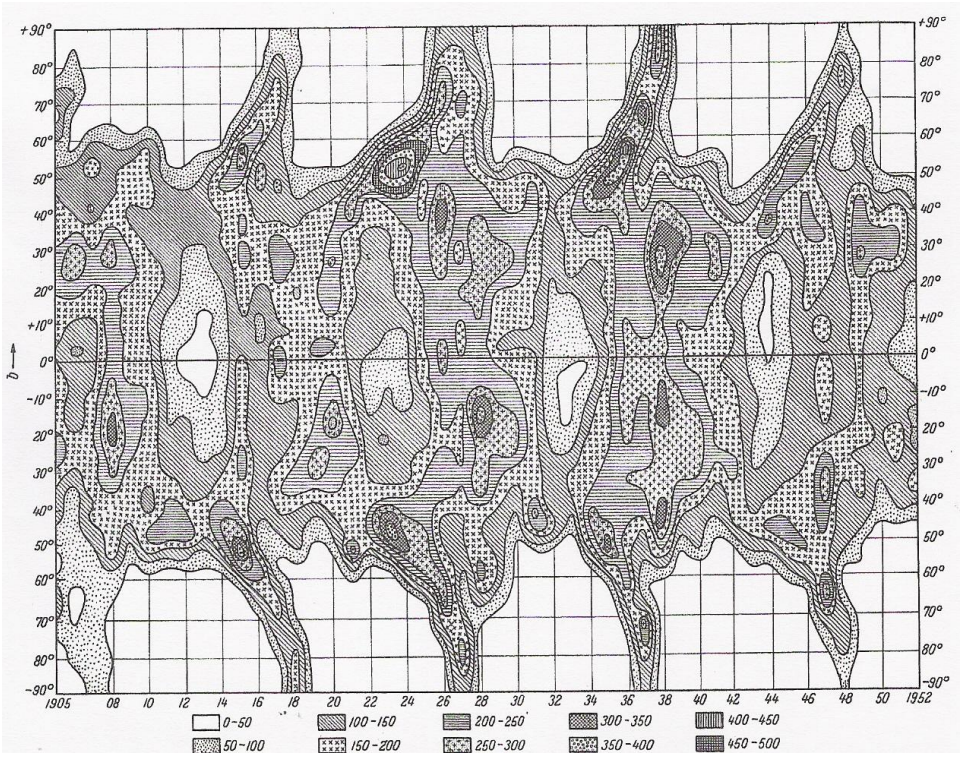

Figure 5. Isopleths of mean daily prominence areas from 1905 – 1952, showing the equatorward drift of low-latitude prominences and the poleward drift of those at high latitudes. From Anathakhrishnan, (1954).

Hence, a large-scale meridional circulation is needed in dynamo models. The existence of this meridional circulation was confirmed by helioseismologic observations. In Section 13 we discuss the implications of the recently observed increased circulation speed (Hathaway and Rightmire, 2010).

9. Proxies and the Phase Diagram; Its Diagnostic Value

We want to have indicators for the variability of the tachocline in order to study its behaviour, thus hoping to further specify the information on the mechanisms at work. Direct observations are possible by means of the technique of helioseismology but these cover only one or two decades and hence they do not give information on the longer term variations. Less direct information can be acquired by measurements of the magnetic fields in polar and equatorial areas of the sun but there the drawback is that the equatorial fields are only known

for the last century and the polar ones even for a shorter period of time. That situation requires the need for 'proxies' of these two magnetic field components.

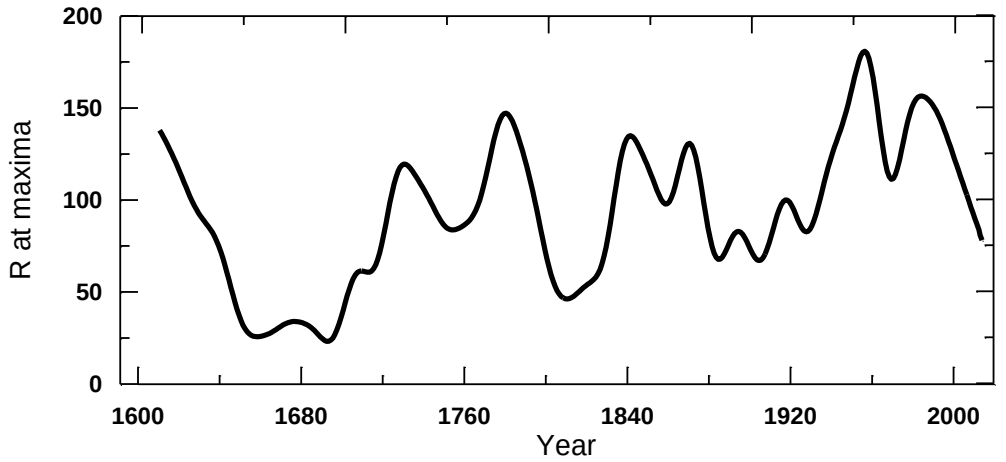

Figure 6. Values of R_{max} since 1610.

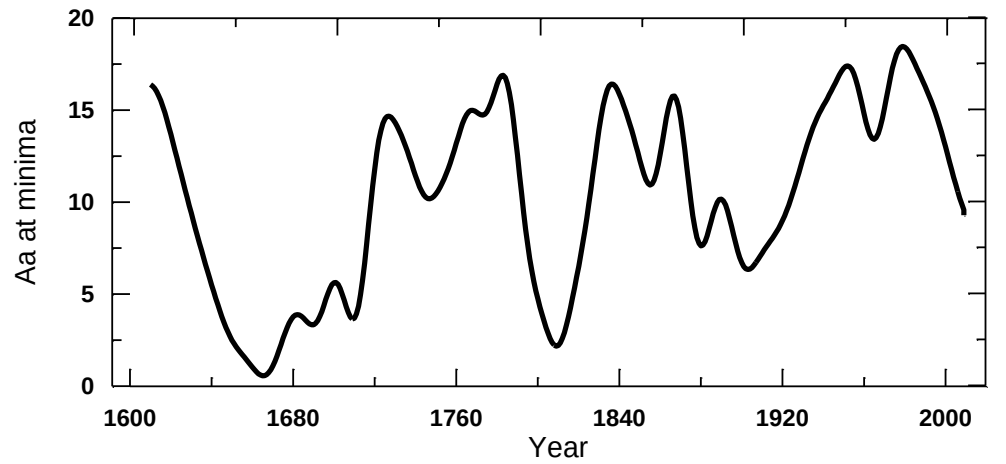

Figure 7. Values of aa_{min} since 1610. Only the part from 1844 onward is based in direct observations; the earlier part is extrapolation (Nagovitsyn, 2006).

A proxy for the toroidal magnetic fieldstrength is given by R_{max}, the maximum number of sunspots in successive Schwabe cycles (Nagovytshin, 2005); cf. Figure 6. It was shown by Russell (1975), Russell and Mulligan (1995), Duhau and Chen (2002) and confirmed by others, that a convenient proxy for the maximum poloidal magnetic fieldstrength is aa_{min}, the minimum value of the *aa* magnetic component. The *aa* data are based on simultaneous measurements of the terrestrial magnetic fieldstrength in Greenwich (UK) and Adelaide (Australia). They exist since 1844 (Mayaud, 1975). A diagram of the aa_{min} values is given in Figure 7. Nagovitsyn (2006) has extrapolated them to earlier years, partly on the basis of an assumed relationship with sunspot numbers. Such extrapolations should always be handled with caution as long as the assumed relationship has not been proven by solid physical theory.

A comparison of these two diagrams shows, first, great similarities and a fairly high degree of correlation between R_{max} and aa_{min}, but next to that there are conspicuous, during the Maunder. These mark those between the toroidal and poloidal field components of the solar dynamo and their study may be important for improving our understanding of the dynamo mechanism. Particularly interesting is the difference between both during the Maunder Minimum. They are shown too in Figure 4. That diagram also shows the differences between the sunspot numbers and the solar particle fluxes, a difference that points to their different origins. We hypothise, that these differences are related to those in the toroidal and poloidal fields respectively. Note also that during the 20th century Grand Maximum the maximal field strength of the toroidal field was reached around 1957 while that of the poloidal field was only reached much later, viz. around 1980 – 1990.

For the study of the time history of the solar tachocline it therefore makes sense to examine the simultaneous variation and the mutual dependence of the two proxies. To that end Duhau and Chen (2002) have introduced a *phase diagram* in which R_{max} is plotted as a function of aa_{min} during the period 1610 to present. Its study gives rise to an interesting conclusion: it appears (Duhau and Chen, 2002; Duhau and De Jager, 2008) that at the time of transition from one Grand Episode to another the Gleissberg-type components of the two proxies take well-defined values, while at the same time two of the oscillations in which the R_{max} time series can be split, are also passing through these well-defined values. These two oscillations are, first, the decadal component, consisting of the lower Gleissberg band and its harmonics and second: the long-term component, based on the upper Gleissberg and the De Vries cycles. This transition point coordinates of the two proxies is given by R_{max} = 93.38 sunspot numbers and aa_{min} = 10.34 nT (Duhau and De Jager, 2008). We call these two values the *parameters of the Transition Point.*

Having thus defined the Transition Point in the phase diagram, it makes obviously sense to plot the values of the two proxies with respect to the Transition Point values, as is done in Figure 8.

This diagram shows the path of the 'Gleissberg cycle' this last defined as the long term component from which the transition point coordinates are subtracted. Figure 8 presents the phase diagrams for two periods, the episode of the Maunder Minimum (M - Figure 8a) and that of the Dalton Minimum.

There were two Gleissberg cycles in the interval 1610-1787. The lengths of these cycles were 157 years of (Figure 8a) and 93 years (Figure 8b). It is perceptible that the Dalton minimum occurs during the episode of Regular Oscillations. The latter is characterized by cycles of moderate amplitude. The Dalton minimum is not distinguishable in that pattern. It reflects a strong oscillation.

It seems to be due to a strong oscillation with a periodicity in the lower Gleissberg band. There are evidences that Maunder and Dalton type minima have different physical origins (Duhau and de Jager, 2010) It is then clear that the phase diagram may also be used as a diagnostic diagram because it opens the way to predicting future transitions between Grand Episodes.

It appears that such transitions occur when the R_{max}, aa_{min} curve in the phase diagram passes through the Transition Point. When it does not exactly hit the Transition Point, then the transition is followed by an episode of Regular Oscillations, as was the case in 1724 (Duhau and De Jager, 2008). We conclude that the length and the strength of these cycles are correlated. This unveils the non-linear nature of the Gleissberg cycle.

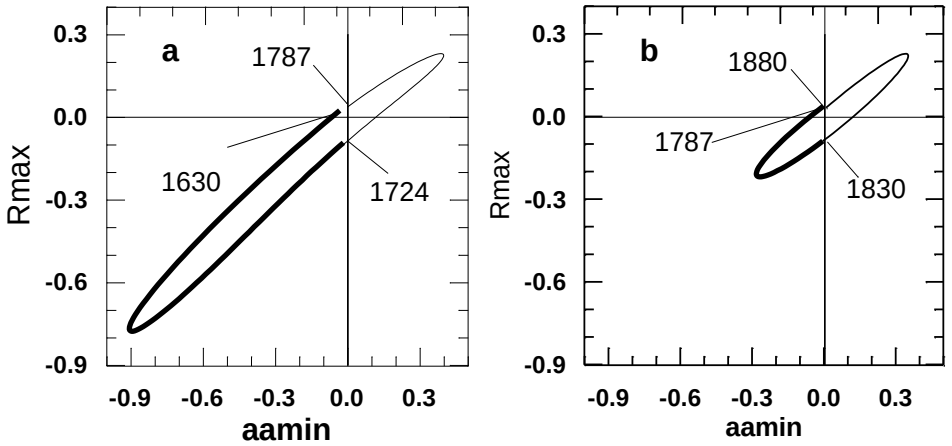

Figure 8. Phase diagram of the Gleissberg cycle during the period 1630 to 1880. The diagrams refer to the Maunder Minimum (1630-1724) and the Dalton Minimum (1787 – 1830) and the 1724-1924 episode of regular oscillations during which the Dalton minimum occurred (1787-1830; thick line in the right panel). Phase transitions to Grand episodes tend to occur when the R_{max}, aa_{min} curve runs through or very nearby the Transition Point.

10. Solar Cycles; Quasi-Harmonic Oscillations and Periodicities; Wavelet Representation; Physical Origin of the Periodicities Beyond the Hale Cycle

We next proceed to a closer study of the solar periodicities and thereby wish to accentuate the difference between the character of periodicities in bound and open systems, in linear and non-linear systems. Specifying the differences is needed for a physical interpretation of the observations. Modes of oscillations of a linear and stationary bound system are harmonics functions, therefore any oscillation in these system is well represented by the Fourier base function,. The same is not true in a non-linear system with a non-stationary boundary for which the modes of oscillation change with time in frequency and in amplitude. For describing oscillations in such a kind of system a base function of compact support is needed. .Here we use the Morlet wavelet representation, to be described below.

In the case of solar variability the important events are those in which the dominant periodicities change abruptly in time (Duhau and De Jager, 2010), which happens during the phase transitions between grand episodes. This indicates that at the time of phase transition an abrupt change in some boundary condition does occur.

During each solar dynamo episode the periodicities of the fluctuations in the strength of the solar magnetic field components of the sunspot cycle around the transition point level are constant but the relative power contained in each of them is not. As a consequence these fluctuations may be split in oscillations that have highly variable amplitudes but nearly constant lengths. We call these oscillations ‘quasi-harmonics’.

This quasi-harmonic behaviour may be visualized in Figure 9 which shows the Morlet wavelet scalogram for 150 years of sunspot number data. Each quasi-harmonic oscillation is displayed there by a succession of dark and lighter areas occurring at nearly regular intervals and covering a band of periods. In the scalogram of Figure 9 we identify four ranges of sunspot numbers whose periods are roughly in the bands: 7 to 15, 15 to 32, 32 to 75, 75-130 and above 130 years. We denote these by the Schwabe, Hale, lower Gleissberg, upper Gleissberg and Suess (De Vries) bands , respectively, since each of them contains one of these well know periodicities (de Jager 2005).

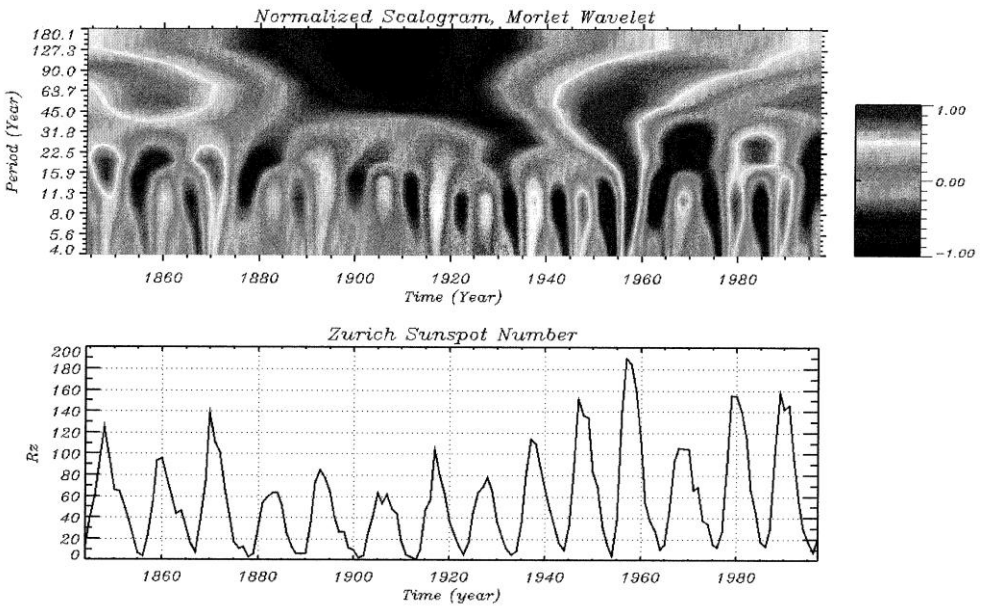

Figure 9: the Morlet wavelet scalogram of the annual mean sunspot number for the last 150 years (copied from Duhau and Chen, 1999).

While the scalogram gives a qualitative idea of the oscillatory behaviour of the time series in the frequency domain, the spectral analysis allows one to study its evolution in this domain in the course of time. In order to understand the nature of each of the quasi-oscillations we also need to represent its path in the phase diagram, for which a splitting of the fluctuation in its quasi--harmonic components in the time domain is needed (Duhau and Chen, 2002, Duhau and de Jager, 2008). The particular base function that may be applied to perform this splitting depends on the nature of the system that sustains the oscillations (see e. g. Kostas et al. 1999). A method for performing it in the case of the solar dynamo, this being a two layered bound system that undergoes sudden changes in its boundary conditions, has been introduced by Duhau and de Jager (2010).

Figure 10 shows the time series of R_{max} and aa_{min}, in which both are normalized with respect to the coordinates of the Transition Point. The vertical co-ordinate gives the amplitudes of the poloidal and toroidal magnetic field components in units of sunspot numbers and nT, respectively:

$$r_{\max} = \frac{R_{\max} - tp_R}{tp_r}, \qquad (1)$$

$$AA_{\min} = \frac{aa_{\min} - tp_{aa}}{tp_{aa}} \qquad (2)$$

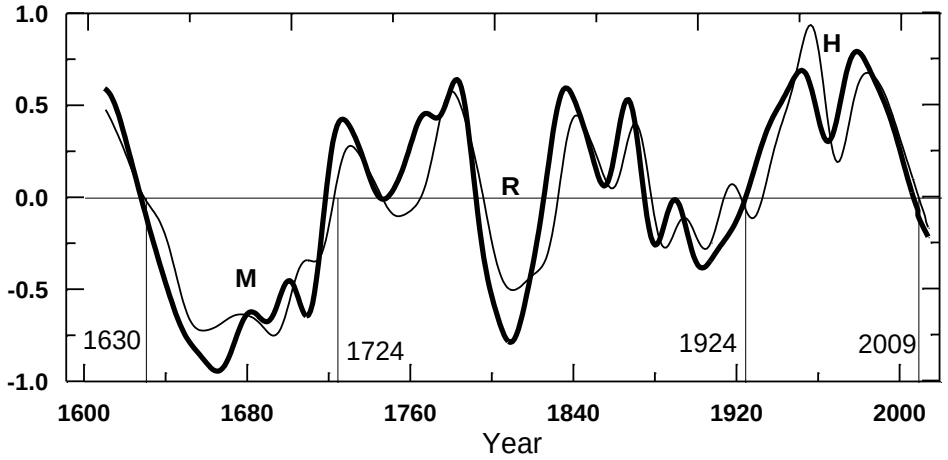

Figure 10. The time-variation of maximum sunspot number R_{max} (thin line) and geomagnetic index minima aa_{min} (thick line) as normalized by equations (1) and (2), respectively. The short vertical lines are plotted at the years of the maxima of the polar cycles for which the phase transitions occur that lead to Grand Episodes viz. the M episode (Maunder Minimum; 1630-1724) the R episode (Regular Oscillations; 1724-1924) and the H episode (High 20th century Maximum; 1924-2009).

Table I. Wavelet Fourier periods of the wavelet components for D = 6, n = 3

Band	Wavelet Fourier periods (years)			
Hale		17.00	21.42	26.98
Lower Gleissberg	34.00	42.84	53.97	68.0
Upper Gleissberg	85.67	107.94	136.0	171.3
Suess (De Vries)	215.9	272.0	342.4	431.8

Table I gives the Fourier periods of the wavelet components of the base functions that allow for an accurate representation of the 400 years long time series. The parameters *D* and *n* that define the base functions in the Table caption are the ratios of the widths of the Gaussian envelope to the Fourier period of each wavelet component and the number of subscales between scales (see Torrence and Compo, 1998). We have defined there four band of periods, according to their dominant periods, viz. the Hale, lower Gleissberg, upper Gleissberg and De Vries (Suess) bands.

A given quasi-harmonic oscillation in the system may contain more that one period. In the case of the signal that we have called Gleissberg cycle it comes from building first the

long-term trend that we have defined as the signal that results form the addition of all the wavelets in the upper Gleissberg band and beyond and the linear trend. We have called 'Gleissberg cycle' the quasi-harmonic oscillation that results from subtracting the constant level from the long term trend because their paths in the phase diagram are closed loops (see figure 8). This cycle may be due to a cyclical oscillation of the spin of the inner radiative core with respect to the convective envelope. Alternatively it is also probable that the lower Gleissberg band, which leads to a semi-secular quasi-harmonic oscillation that we have called 'semi-secular' has a completely different meaning since it is most likely due to torsional oscillations of the tachocline. The superposition of the wavelet components in the Hale band (see table I) causes an oscillation. This is the first quasi-harmonic of the semi-secular oscillation. We will call it the bi-decadal oscillation. The semi-secular and the bi-decadal oscillations seem to be linked to the symmetrical and anti symmetrical parts, with respect to the solar equator respectively, of an identical phenomenon, probably to be ascribed to torsional oscillations in the tachocline. Because of mass and angular momentum conservation they must be visible too in the meridional flux (see e. g. Shibahashi, 2006).

In Section 2 of this paper we referred to the various observed cycles by their conventional names: Hale, Gleissberg, De Vries, Hallstadt. These names originated 'historically'. But it is clear from the preceding analysis that these 'cycles' or better 'periodicities' have various components (cf. Table I) and these ask for a physical interpretation. The semi-secular cycle and its first harmonic, the bi-decadal one, may be safely called a torsional cycle. Allocating a physical interpretation to the – variable – Gleissberg cycle is more difficult but most probable we may call this cycle: inertial spin cycle, because it seems to find its basis in the oscillation of the spin of both the inner core and the convective envelop (because of angular momentum conservation) in the inertial reference coordinates.

The bi-decadal torsional oscillation has its dominant periodicities in the Hale band. Observations indicate that the meridional turnover time and the Hale cycle were synchronic during the last few cycles and the hypothesis has been forwarded that the meridional turnover time is fixing the Hale cycle length (Hataway, 2003, Dikpati, et al., 2004). However, during the current transition the length of the bi-secular oscillation would increase from its 21 year value that prevailed after 1888 (during which the strongest change of phase of the last 400 years occurred – compare Figures 8 and 9 – to 32 years. In this case the synchronicity would be lost since the Hale cycle length would stay near 22 years. In case this would be confirmed we would have indications that the Hale cycle and the bi-secular oscillation are due to different phenomena in the solar dynamo. While the first originates in the tachocline level by a magnetohydrodynamic wave, the second is the N/S asymmetric signature of torsional oscillations at the tachocline level, that are accompanied by a meridional flux with the same periodicity. The above considerations, evidently need further study and confirmation.

11. Forecasting Schwabe Cycle 24 - Late and Low; Comparison with Other Forecasts

A brief review of predictions of the amplitude and time of maximum of the next Schwabe cycle, #24, is given by De Jager and Duhau (2009a), and based on a review by Pesnell (2007). The nearly 50 forecasts mentioned there show a bewildering diversity. A NOAA-NASA

panel of 13 members and 8 consultants came with a split opinion: Cycle #24 might either peak in October 2011 with R_{max} = 140 ± 20 or either in August 2013 with R_{max} = 90 ± 10. One of the reasons for this divergence is that most of the methods used (reviews by Hathaway et al. 1999; Schatten and Hoyt, 1998) assume the relation between the parameters involved to be linear. But the solar dynamo is a non-linear system.

We describe the forecast by De Jager and Duhau (2009a). It is based on a discussion of several relationships, cf. also Olh (1966), Legrand and Simon (1989) and Simon and Legrand (1989). One is that between the observed average polar magnetic field strength DM (Svalgaard et al. 2005) and the aa_{min} value (Figure 11). This diagram allows one to forecast aa_{min} a few years in advance of the next solar minimum and at the same time it quantifies aa_{min} in terms of the polar cycle. From data in Figure 11 it was concluded that the most likely value for aa_{min} during the sunspot minimum is aa_{min} = 9.8 ± 1.2 nT.

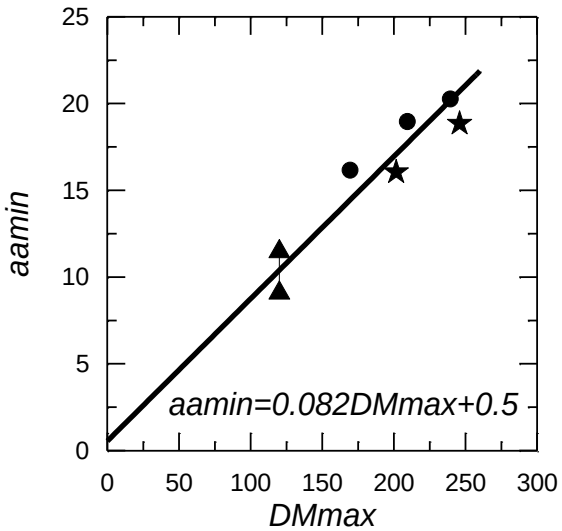

Figure 11. Values of aa_{min} as a function of DMmax (De Jager and Duhau, 2009a).

At the time of writing this review we are now able to check that forecast. Figure 12 compares observed *aa* values for the pair of cycles #16 and #17 during which the 1924 transition occurred, with the pair that is presently under discussion: ## 23 and 24, during which a new transition to a deep minimum is expected. The horizontal full lines indicate the twelve months that have been considered when computing the minima of the 12 months moving average of the geomagnetic index between the two consecutive cycles as quoted in the left corner of the panels. These average values are proxies for the strength of the polar cycles between each of the pairs

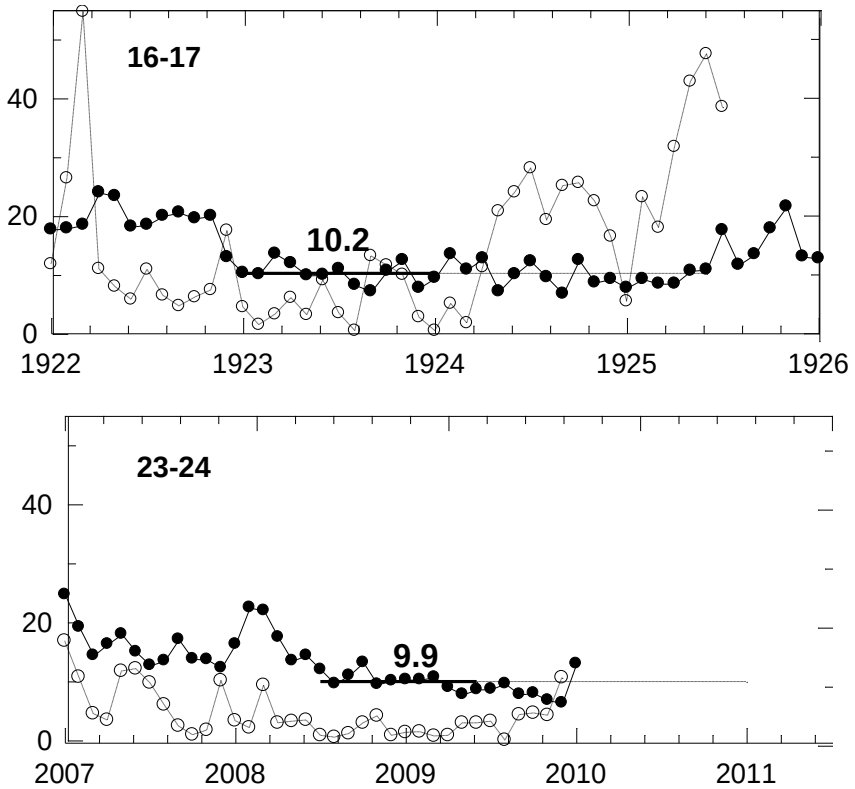

Figure 12. Sunspot number (open circles) and geomagnetic index (filled circles) monthly means and the minimum of the 12 months moving average of the geomagnetic index aa at sunspot minimum between the pairs of cycles indicate in the respective figures. The horizontal lines indicate the 12 months interval for which the quoted average value is computed (full line) and the additional interval during which the monthly values stabilizes around that minimum (dashed line).

It is apparent from Figure 12 that at sunspot minimum values of the *aa* geomagnetic monthly means undergo small oscillations around a minimum value. In the case of the 1924 transition (upper panel) this behaviour started when the sunspot number had reached values near zero and it lasted for two and a half years (see the dashed horizontal line). Consequently it lasted for more than a year prior to and for more than a year after the date at which the sunspot number started its sharp increase at the onset of the new cycle. During the 2009 transition the behaviour appears to be similar to that during the 1924 transition, with the difference that the sunspot number remains conspicuously close to zero during a fairly long time span. We expect (cf. the next Section) a fundamental difference between the 1923 transition to a Grand Maximum and the present transition, presumably to a Grand Minimum.

It is gratifying to observe that the value of aa_{min} during the 2009 transition, 9.9 nT, agrees very well with the value predicted by de Jager and Duhau (2009a), 9.8 ± 1.2 . This value is slightly below the average value of the ordinate of the Transition Point, 10.3 ± 0.08 that was derived from the five phase transitions that have occurred during the last millennium (Duhau and De Jager, 2008). However, the values of the transition coordinates for the five phase transition occurring during the last millennium have been obtained from yearly means values of the corresponding time series but in figure 12 and in the prediction by De Jager and Duhau (2009a) a 12 months moving average is used instead.

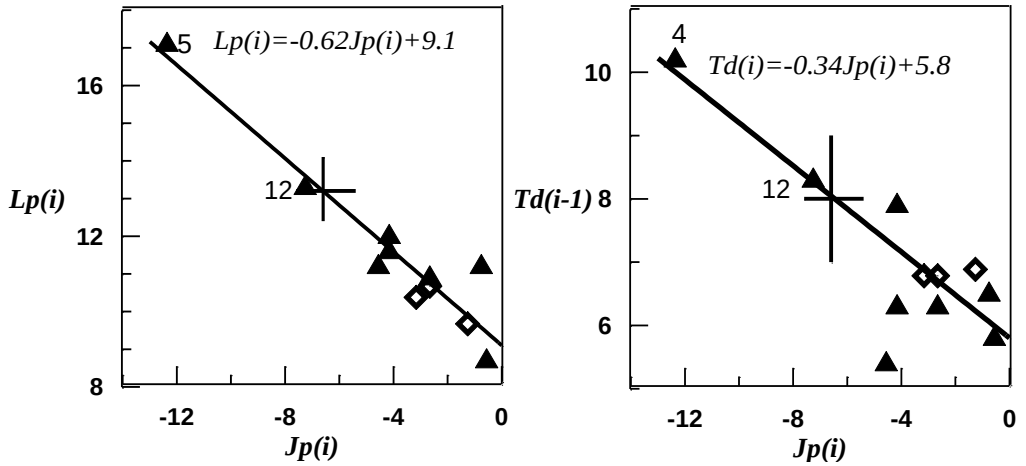

Figure 13. 'Lengths of the polar cycles # *i* (left) and the decaying time of sunspot cycles # (*i-1*) (right) plotted against the amplitude difference between the two consecutive polar cycles (see also the text). The plusses are the predicted values for the length of polar cycle # 24 and for the decaying time of sunspot cycle # 23 (from De Jager and Duhau, 2009a).

To proceed further with forecasting the next maximum and the time of occurrence we show in Figure 13 two diagrams. They refer to consecutive polar cycles, in which the length of the polar cycle is defined as the time difference between subsequent aa_{min} values. In both of them the abscissa is the difference between the amplitudes, as measured by aa_{min} of two consecutive polar cycles. The left panel gives the length of the relevant polar cycle and the right-hand one the time difference between the maxima of the two sunspot cycles involved. These diagrams allow us to determine the time of the next Schwabe cycle maximum as soon as the length of the polar cycle is known. The predicted length of the polar cycle (Figure 13 left) is 13.2 ± 0.6 years, as sunspot maximum 23 in the monthly smoothed values occurred at 2000.8. Hence, sunspot maximum #24 is predicted to occurs in 2014.0 ± 0.6. To check these considerations we 'forecast' the length of the period between the minima of sunspot cycles #23 and #24 (cf. the cross in Figure 13 right). It appears to be 8 ± 1years. Hence, the expected time of occurrence of that minimum is 2008.8 ± 1 which is within the observational limits is in agreement with the observed one (see figure 12).

The sunspot number value at sunspot maximum #24 was predicted to be R_{max} = 68 ±17 (De Jager and Duhau, 2009a) .This prediction was based in the characteristics of an R type episode. However, a prediction made with a new homogenized time series of Lockwood et al.(priv. comm., 2009) leads instead to the expectation that the forthcoming episode would be of the M (Maunder) type and in that case R_{max} = 55 (Duhau and De Jager, 2010).

Concluding, we foresee a late (2014) and low (R_{max} = 68) solar maximum for Schwabe cycle #24.

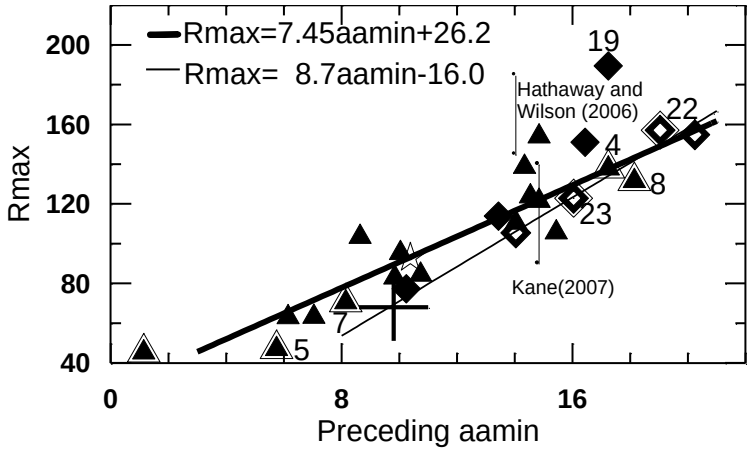

Figure 14. Empirical relation between R_{max} and aa_{min} and comparison with similar data from other investigators (cf. de legends in the diagram). The cross refers to the aa_{min} data during the 2008 -2009 minimum, i.e. between cycles #23 and #24. (From De Jager and Duhau, 2009a).

12. FORECASTING THE NEXT GRAND EPISODE – A MAUNDER-TYPE MINIMUM?

Here we study the longer-term behaviour of the sun's activity. To that end we again consider the diagnostic phase diagram of Figure 8. We found (Duhau and De Jager, 2008) that a transition to another episode occurs when the R_{max}, aa_{min} curve in that diagram passes close to the Transition Point, TP). When it *precisely* crosses the TP a Grand Maximum or Grand Minimum is immanent. When it passes the TP at some distance the transition will be followed by an episode of Regular Oscillations, as happened in 1743. A yet unanswered question is how close it should pass in either case.

The standard values of the geomagnetic index *aa* were recently corrected by Lockwood et al. (2009). This new *aa* time series, aa_c starts in 1868. We have used these improved data for deriving an improved phase diagrams of the Gleissberg cycle than in our earlier study (De Jager and Duhau, 2009a, improved in Duhau and De Jager, 2010). It is shown in Figure 15 and it shows a remarkable behaviour when compared to those for the earlier periods as the one shown in Figure 8. It represents a perfect correlation between R_{max} and aa_{min}. We note that in the year 2009 the Gleissberg cycle exactly crossed the Transition Point.

So far we have described three cases, those of 1880, 1924 and 2009. In each of these the Gleissberg cycle passed nearly or even fully through the Transition Point on its return way. This behaviour was quite different in 1880 and 1924 but there is remarkable similarity between the 1924 and the 2009 cases. Since there are indications (De Jager and Duhau, 2009a, and the preceding section of this paper) that the Grand Maximum ended in 2009 we conclude that after the current polar magnetic cycle a transition is immanent towards a Grand Minimum

A transition directly from a Grand Maximum to a Grand Minimum occurred only once in the last millennium (see figure 4b in Duhau and de Jager, 2008). This happened in the 14th century, in a transition from the so-called H episode to the Suess Minimum.

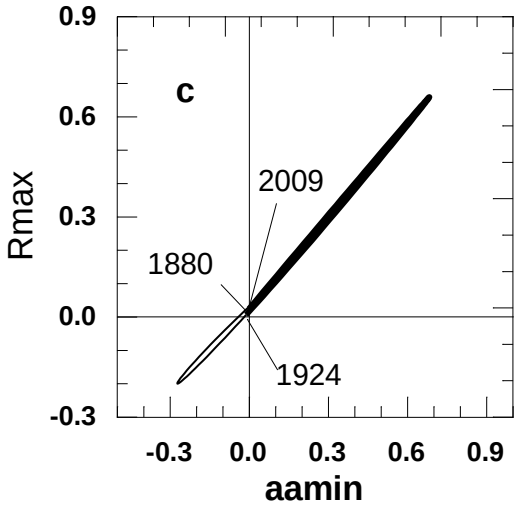

Figure 15. The remarkable phase diagram for the period 1880 to 2009 of the Gleissberg cycle, as obtained from the new homogenised time series of geomagnetic index aa_c as presented by Lockwood et al. (priv. comm.. 2009).

The two successive sunspot maxima around that transition, as seen in Schove's (1955) sunspot maxima, were in 1402 and 1413. Hence, the corresponding polar cycle was about 11 years. On the other hand, the present polar cycle may appear to be as long as 14 years as estimated by de Jager and Duhau (2009a) and elaborated in the preceding section of this paper. Therefore, the polar cycle #24 is expected to be similar to that of cycle #12. Both have in their positive phase strong decadal oscillations that, in the case of cycle #12, were followed by the Dalton Minimum.

However, a sharp change of phase may occur in the decadal oscillations, as was the case after 1921. The uncertainty that we meet here is a consequence of the short horizon of predictability that belongs to phenomena in the decadal time scale. A study of the Lyapunov exponents (Ostriakov and Usoskin, 1990; Sello, 2001, 2003) shows that solar activity can be predicted only a few years in advance.

Support for the above conclusions about the immanence of a Grand Minimum is found in Makarov et al. (2010) who showed that the rest latitudes of the sunspot bands gradually tended to decrease during the past few decades (Figure 16).

That phenomenon was interpreted by the authors as an indication that a Grand Minimum could start around 2020 ~ 2030. The present situation may be compared with that around 1630 (see Figure 1), where the Maunder minimum was preceded by increasingly weaker Schwabe cycles.

The remarkable decline of the average sunspot fieldstrength, initially found by Penn and Livingston (2006) and confirmed by Livingston and Penn (2009), and seen as an indication of forthcoming strong changes in solar activity, was later denied by Schad and Penn (2010).

Conclusion: Solar activity is presently going through a brief period of transition (2000 – 2014). This transition period will be followed by a Grand Minimum, most likely of the Maunder type and most probably to start in the twenties of the present century.

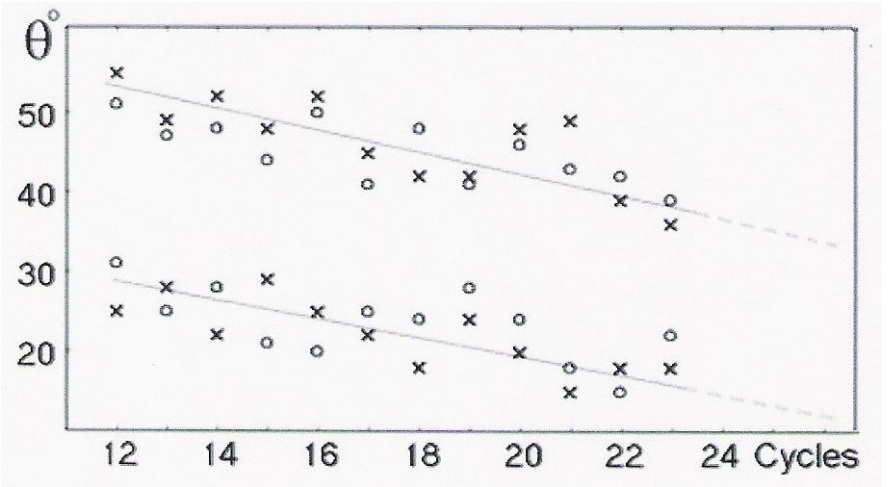

Figure 16. Decreasing latitude of sunspot bands in the course of the last few decades (Makarov et al, 2010).

13. Dependence of Global Surface Temperature on Solar Activity

The problem we wish to touch here is that of the dependence of terrestrial surface temperatures on solar activity. Several authors have dealt with this problem and derived correlations of different amount. Recently Johnson (2010) found that the terrestrial surface temperature correlated well with solar activity for the years 1610 – 1990. In two other recent papers (De Jager and Duhau, 2009b; De Jager, Duhau and Van Geel, 2010) similar results were found. That there must be a relation is evident from the observation that the temperature *T* increased gradually from the Maunder Minimum till the 20th century Grand Maximum. The same applies to R_{max} as indicated by Figure 3 and by Figure 1 of De Jager and Duhau (2009b). It also applies to aa_{min} (Figure 3 of De Jager and Duhau, 2009b). So far all authors who discussed sun-temperature relations studied the correlation between terrestrial surface temperatures and the solar equatorial magnetic field, approximated by the number of sunspots. But since the polar magnetic flux is at least as strong as the equatorial one there is no reason to neglect the polar fields.

In that line we (De Jager, Duhau and van Geel, 1010), by assuming this relationship to be linear, which is the simplest assumption in the absence of a physical theory, wrote:

$$T = x \cdot R_{max} + y \cdot aa_{min} + z \cdot time + const \qquad (2)$$

In this expression z is the temperature gradient that is not correlated with solar variability. Hence, we determine the constants *x, y* and *z* in such a way that the resulting fit follows the interdecadal variations, and we investigate how much of the secular *T* rise can be accounted for. To simplify the calculations, the R_{max} and aa_{min} data were normalized to the Transition Point coordinates in the phase diagram (cf. eq. (1a) and (1b) and Figure 8; cf. also De Jager

and Duhau, 2009b; De Jager, Duhau and Van Geel, 2010). Since the R_{max} and aa_{min} values are normalized, the units of x and y are ^{o}C. That of z is ^{o}C/century.

The investigation was applied to the seven temperature data sets that were used previously by De Jager and Usoskin (2006) and De Jager and Duhau (2009b). It soon appeared that a direct analysis, based on the classical least squares method yielded unreliable results, because aa_{min} and R_{max} are correlated to a fairly large degree. That was a weakness in De Jager and Duhau (2009b) and it produced an uncertain result. In De Jager, Duhau and Van Geel (2010) a more subtle line of attack was followed, working in two opposite approaches.

In our first step we write

$$T = x \, . \, R_{max} + const \, ,$$

hence neglecting for the time being the y and z terms, and we determined x by least squares for the period for which sunspot data are available:1619 to 1970. Thereafter we determined y and *const* for data covering the period 1844 – 1970, by a least squares analysis of

$$T - x \, . \, R_{max} = y. \, aa_{min} + const$$

Having thus found x and y in first approximation we tried to improve them by successive iterations, repeating the procedure for the residuals. It turned out that two iteration steps were as a rule sufficient. More iteration steps did not improve the results but they did increase the resulting mean errors.

In the second step we went the other way round by first determining y from

$$T = y. \, aa_{min} + const$$

We did this for the period for which *aa*-data are available: 1844 – 1970. Thereafter x was determined, similarly and complimentary to the above treatment.

The weighted averages of the results, weighted according to the inverse squared mean errors, are: $\langle x \rangle = 0.3595 \pm .0071$; $\langle y \rangle = -.1851 \pm .0086$. Hence, $y/x = -0.5194$. We judge the accuracy of the data by deriving the ratios of average values $\langle \mu_x \rangle / \langle x \rangle = 0.02$ and $\langle \mu_y \rangle / \langle y \rangle .= 0.22$. These values give some confidence in the data. For the gradients, z and z_0 we found $\langle z_0 \rangle = 0.0868 \pm .0030$ and $\langle z \rangle = 0.0508 \pm .0020$. Further, the ratio of the sun-correlated gradient over the total gradient is $\langle (z_0 - z)/z_0 \rangle = .454 \pm .018$, and $(\langle z_0 \rangle - \langle z \rangle) / \langle z_0 \rangle = 0.415$. The difference between the two last numbers is satisfactorily small; the average is 0.43.

In conclusion: the average gradient of the tropospheric temperature during the period 1619 – 1970 was $\langle z_0 \rangle = 0.0868 \pm 0.0030$ ^{o}C/century. The fraction 0.43, being 0.037 ^{o}C /century was correlated with solar variability. The average temperature gradient correlated with the *equatorial field component* is 0.077 ^{o}C /century. Satisfactorily, this component can fully be explained by the gradual increase of the Total Solar Irradiance if one includes the feedback by water vapour greenhouse effects (Bony et al., 2006; see also Murphy et al., 2009).

The temperature component, correlated with the *polar field component* appears to be – 0.040 ^{o}C/century. The minus sign of the *y* value tells that sun-induced warming due to the poloidal field component is strongest for weakest poloidal fields. The increase correlated with the poloidal field component may be related to the strong solar wind at polar maximum but the physical explanation is still an open challenge. The suggested relation between cosmic rays and cloud formation is not confirmed by Kulmala et al. (2010).

The *residual non-solar* global temperature gradient, hence obtained after having subtracted the solar part and presumably to be ascribed to climatologic causes is 0.051 ^{o}C/century. We note the suggestion by Akasofu (2010) who ascribes it to the non-linear recovery of our atmosphere from the Little Ice Age and the multi-decadal oscillation.

A final question refers to the surface temperature during a forthcoming Maunder-type Minimum. From the above results we derive that it would cause – during the central time of the Minimum – a relative decrease in the temperature of ~ 0.4 ^{o}C. This result is comparable to that of Feulner and Rahmstorf (2010) who found 0.3 ^{o}C.

CONCLUSIONS

We described solar variability and its many manifestations. The various *solar cycles* show the various periodicities. There are three kinds of longer lasting *grand episodes*: the Grand Maxima (example: the 20th century maximum: 1924 - 2009); Grand Minima (example: the Maunder Minimum: 1630 -1743), the episode of Regular oscillations: 1743 – 1924). Their behaviour can be described by a *phase diagram* with a good diagnostic value. We extensively summarize the physics of the tachocline, this being the seat of solar variability. The Hale cycle of average 22 years duration is ascribed to magnetohydrodynamic pulsations of (part of) the tachocline.

Based on the foregoing we forecast the next '11-years' (Schwabe) cycle. We expect a late (2014) and low (sunspot number 55) next maximum. It will be the onset of another Grand Minimum, expected to begin in the twenties of the present century.

We studied the relation between average terrestrial surface temperature and solar variability for the period 1610 – 1970. During this period the average terrestrial surface temperatures are correlated both with the equatorial as well as the polar solar magnetic field components. The correlation with the equatorial field can fully be explained. It is due to the gradual increase of the Total Solar irradiance and the consequent feedback by evaporated gases. The explanation of the polar correlation is still open.

In the period of study there was a remaining presumably atmospheric component.

After subtraction of the solar and terrestrial components from the recent temperature increase there remains residual warming; its smoothed values attained a value of 0.31 ^{o}C in 1999.

ACKNOWLEDGMENTS

We are greatly obliged to. D.K. Callebaut, both for his critical comments on two earlier versions of the paper and for his helpful suggestions for improvement.

REFERENCES

Akasofu, S.I., Watanabe, H., Saito, T.:2005; *Space Sci. Rev*. 120, 27.

Akasofu, S.I., 2010, *J. Atm. And Solar-Terrestrial Phys*., submitted.

Ananthakhrishnan, R.: 1954, *Proc. Indian Acad. Sci*. 49, 72.

Bahcall, J., Ulrich, R.: 1971, *Astrophys. J.* 170, 593.

Basu, S.: 1997, *Mon. Not. R. Astron. Soc.* 288, 572.

Bazilevskaya, G.A., Krainev, M.B., Makhmutov, V.S.: 2000, *J. Atm. Sol. Terr. Phys*. 62, in the press.

Benevolenskaya, E.J.: 2003, *Solar Phys*. 181, 237.

Berdyugina, S. V., Braun, P. A., Fluri, D. M., Solanki, S. K.: 2005, *Astron. Astrophys*. 444, 947.

Bonanno, A., Elstner, D., Rudiger, G., Belvedere, G.: 2002, *Astron. Atrophys*. 390, 673.

Bony,S., Colman, R., Kattsof, V.M., Allan, R.P., Bretherson, C.S., Dufresne, J.-L., Hall, A., Hallegatte, S., Holland, M.M., Ingram, W., Randall, D.A., Soden, B.J., Tselioudis, G., Webb, M.J.: 2006, *J. of Climate* 19, 3445.

Bravo , S., Steward, G. : 1995, *Ast. J.*, 446,431-434.

Bravo, S.; Stewart, G. A.; Blanco-Cano, X.:1998, *Solar Phys*. 179, 223.

Brun, A.S.: 2004, *Solar Phys*. 220, 333.

Caligari, P., Moreno-Insertis, F., Schussler, M.1995, *Astrophys. J.* 441, 886.

Callebaut, D.K., Makarov, V.I., 1992, *Solar Phys*. 141, 381.

Callebaut, D. K. and Khater, A. H. : 2006, in V. Bothmer and A. A.Hady (eds.) Proc. IAU Symposium 233, 'Solar Activity and its Magnetic Origin' Cambridge Univ. Press, ISSN 1743-9213, p. 9-16.

Charbonneau, P.; MacGregor, K. B: 1992, *Astrophys. J*. 397, L63.

Charbonneau, P.; MacGregor, K. B: 1993, *Astrophys. J.* 403, L. 87.

Cliverd, M.A., Clarke, C., Risbeth, H., Clark, T.D.G., Ulrich, T.: 2003, *Astron. Geophys*. 44, 5.20.

Cowling, T.G.: 1945, *Mon. Not. R. Astron. Soc*. 105, 167.

Damon, P.E., Sonnett, C.P.: 1991, in 'The sun in time (A92-46664 19-92)'. University of Arizona Press, p. 360-388.

Damon, P.E., Peristikh, A.N.: 1999, *Geophys. Res. Lett*. 26,2469.

Damon, P.E., Peristikh, A.N.: 2000, *Radiocarbon* 42, 137.

De Jager, C.: 2005, *Space Sci. Rev*. 120, 197.

De Jager, C., Duhau, S.: 2009a, *J. Atm. and Solar-Terr. Phys*. 71, 194.

De Jager, C., Duhau, S.: 2009b, *J. Atm. and Solar-Terr. Phys*. 71, 239.

De Jager, C., Duhau, S., van Geel, B: 2010, *J. Atm. Solar-Terr. Phys*., under review.

De Jager, C. Usoskin, I.G.: 2006, *J. Atm. Sol.-Terr. Phys*. 68, 2003.

Dikpati, M., Charbonneau, P.: 1999, *Astrophys. J.* 518, 508.

Dikpati, M., Gilman, P.A.: 2001, *Astrphys. J.* 559, 428.

Dikpati, M., Gilman, P.A.: 2007, *Solar Phys*. 241, 1.

Dikpati, M., de Toma, G., Gilman, P.A., Arge Ch., White, O.R.: 2004, *Astrophys. J.* 601, 1136.

Duhau, S., Chen, C.:1999, *Annales AFA* (Argentinian Physical Association), 11, 62.

Duhau, S., Chen, C.: 2002, *Geophys. Res. Lett*. 29, 1628.

Duhau, S., De Jager, C.: 2008, *Solar Phys*. 250,1.
Duhau, S., De Jager, C.: 2010, *J. of Cosmetology*, 8, 1983.
D'Silva, S., Chaudhuri, A.R.: 1993 *Astron. Astrophys*. 272, 621.
Eddy, J.A.: 1976, *Science*, 192, 1189-1192.
Feulner, G., Rahmstorf, S.: 2010, *Geophys. Res. Lett*. 37, L05707.
Forgács-dajka, E: 2000, *Astrn. Astrophys*. 413, 1143.
Forgács-dajka, E., Petrovay, P: 2001, *Sol. Phys*. 203, 195.
Forgács-dajka, E., Petrovay, P: 2002, *Astrn. Astrophys*. 389,629.
Friedland, A. and Gruzinov, A: 2003, *Astroparticle Phys* 19, 575.
Gaizauskas, V.; Harvey, K. L.; Harvey, J. W.; Zwaan, C.: 1983, *Astrophys. J*. 265,1056.
Gilman, P.A.: 2000, *Sol. Phys*. 192, 27.
Gilman, P.A., Dikpati, M.: 2000, *Astrophys. J*. 528,552.
Gleissberg, W.: 1944, *Terr. Magn. Atmosph. Electricity* 49,243.
Gleissberg, W.: 1958, *Z. für Astrophys*. 46, 219.
Gnevyshev, M.N., Olh, A.I.: 1948, *Astronom. Zhurn*. 25, 18.
Hathaway, D. Rightmire, L.: 2010, Science 327, 1350.
Hathaway, D.H., Wilson, R.M., Reichmann, E.J.: 1999 *J. Geophys. Res*. 104, 22375388.
Johnson, R.W.: 2010, *Astrophys. Space Sci*. 326, 181-189.
Kosovichev, A.G.: 1996, *Astrophys. J*. 469, L61.
Kostas D. Kokkotas and Bernd G. Schmidt Quasi-Normal Modes of Stars and Black Holes" in Living Revies on Realtivity (http://relativity.livingreviews.org/Articles/lrr-1999-2/).
Krirova, N.A., Solanki, S.K.: 2002, *Astron. Astrophys*. 394, 701.
Kulmala, M., Riipinen, I., Nieminen, T., Hulkkonen, M., Sogacheva, L., Manninen, H.E., Paasonen, P., Petäljä, T., Dal Maso, M., Aalto, P.P., Virjanen, A., Usoskin, I., Vainio, R., Mirme, S., Mirme, A., Minikin, A., Petzold, A., Hörrak, U., Plasz-Dülmer, C., Birmili, W., Kerminen, V.-M., 2010, *Atm. Chem. Phys*. 10, 1885.
Le, G.M., Wang, J.-L.,: 2003, *Chines J. Astron. Astrophys*. 3, 391.
Legrand J-P., Simon, P.A.: 1989, *Annales Geophysicae*, 7 (6), 565-578, 1989.
Lillo, F.: 2005, *Physica* A 349, 667.
Livingston, B.W., Penn, M.: 2009, EOS 90, 257-264.
Makarov, V.I., Makarova, V.V.: 1999, *Proc. 9th European Meeting on Solar Physics*, ESA SP 448, ed. A.P. Wilson, p. 121.
Makarov, V.I., Makarova, V.V., Callebaut, D.K.: 2010, 'Links between polar and sunspot activities', preprint.
Mayaud, P.N.: 1975, *J. Geophys. Res*. 80, 111.
Mestel, L.; Weiss, N. O.:1987, *Mon. Not. R. Asron. Soc*. 226, 123.
Moreno-Insertis, F.: 1994, in M. Schüssler and W. Schmidt (eds) Solar Magnetic fields, Cambridge Univ. Press.
Moreno-Insertis, F.; Caligari, P.; Schuessler, M.: 1995, *Astrophys. J*. 452, 894.
Murphy, D.M., Solomon, S., Portmann, R.W., Rosenlof, K.H., Forster, P.M., Wong, T.: 2009, *J. Geophys. Res*. 114, D17107.
Muscheler,R. Beer, J., Kromer, B.: 2003, in Wu, S.T., Obridko, V., Schmieder, B., Sykora, J. (eds) *ICSI Symposium 2003, ESTEC Noordwijk* , p. 305.
Muscheler, R., Beer, J., Vonmoos, M.: 2004, *Quaterni. Sci. Rev*. 23, 2101.
Nagovytshin, Yu.A.: 2006, *Astron. Lett*. 32, 344.
Nandy, D.: 2002, *Astrophys. Space Sci.*, 282, 209.

Ogurtsov, M.G., Nagovitsyn, Yu., Kocharov, G.E., Jungner, H.: 2002, *Solar Phys*. 211, 371.
Olh, A. I: 1966, *Solnice Danie*, 12, 84-85, 1966.
Ostriakov, V. M.; Usoskin, I. G.: 1990, *Sol. Phys.* 127, 405.
Parker, E.N.: 1993, *Astrophys. J*. 408,707.
Penn, M., Livingston, B.W.: 2006, *Astrophys. J*. 649, L45-L48.
Pesnell, W.D.: 2007, www.swpc.noaa.gov/SolarCycle/SC24/April_16_2007_table.pdf.
Petrovay, K.; Forgács-dajka, E.:2003, Sol. Phys. 205, 39: Raspopov, O.M., Dergachev, V.A., Kolström, T.: 2004, Paleo209,127.
Russell, C.T.: 1975, *Solar Phys*. 42, 259.
Russell, C.T., Mulligan, T.: 1995, *Geophys. Res. Lett*. 22, 328.
Ruzmaikin, A.: 2000, Solar Phys. 192, 49.
Ruzmaikin, A.: 2001, *Space Sci. Rev*. 95, 43.
Ruzmaikin, A.; Feynman, J.; Neugebauer, M.; Smith, E. J.: 2001, *J. Geophys. Res*. 106, A5, 8363.
Schad, T.A., Penn, M.J.: 2010, *Solar Phys.* 262, 19-33.
Schatten, K., Hoyt, D.V.: 1998, *Geophys. Res. Lett*. 25, 599.
Schmitt, D., Schüssler, M. Ferriz-Mas, A.: 1996, *Astron. Astrophys*. 311, L1-L4.
Schove, D.J.: 1955, *J. Geophys. Res*. 60, 127.
Sello, S.: 2001, *New Astron*. 8, 105.
Sello, S.: 2003, *Astron. Astrophys*. 377, 312.
Shibahashi, H.: 2006, *Astron. Nachr/AN*. 999, 789.
Simon P.A., Legrand, J.P.: 1989, *Annales Geophysicae*, 7, (6), 579-594, 1989.
Song, W., Wang, J.: 2005, *Progr. in Astron*. 23, 205.
Soon, W.W., Yaskell, S.H.: 2003, *The Maunder Minimum and the variable sun-earth connection*, World Scientific Publishing, Singapore.
Sonnett, C. P: 1983, *Nature*, 306, 671-673.
Spiegel, E.A., Zahn, J.-P.: 1990, *Astron. Astrophys*. 265, 106.
Svalgaard, L., Cliver, E.W., Kamide, Y., 2006, *Geophys. Res. Lett*. 32, L01104.
Tobias, S.M., Weiss, N.O., Beer, J.: 2004, *Astron. Geophys*. 45, 2.6.
Usoskin, I. G.; Berdyugina, S. V.; Poutanen, J.:2005, *Astron. Astrophys*. 441, 34.
Usoskin. I. G., Valtonen, R., Tanskanen, P.J., Aurela, A.M.: 2009, *Astrophys, J.* 700, L154.
Usoskin, I.G., Solanki, S.K., Schüssler, M., Alanko, K.: 2003, *Phys. Rev. Lett*. 91, 211101-1.
Wagner, G., Laj, C., Beer, J.; Kissel, C.; Muscheler, R.; Masarik, J.; Synal, H.-A.:2001, *Earth Plan. Sci. Lett*. 193, 2001.